Universität Zürich[UZH]

Numerical simulations of shock waves in multiphase mixtures

Tulin Kaman , Remi Abgrall [1]

Institute of Mathematics, University of Zurich

Institute of Computational Science Seminar
16 December 2016

1. With thanks to James Glimm from Stony Brook University

Outline

Problem statement

Consider a flow liquid/bubbles (vapor, air, etc).

An aircraft flying at transonic speeds

Problem statement

Consider a flow liquid/bubbles (vapor, air, etc).

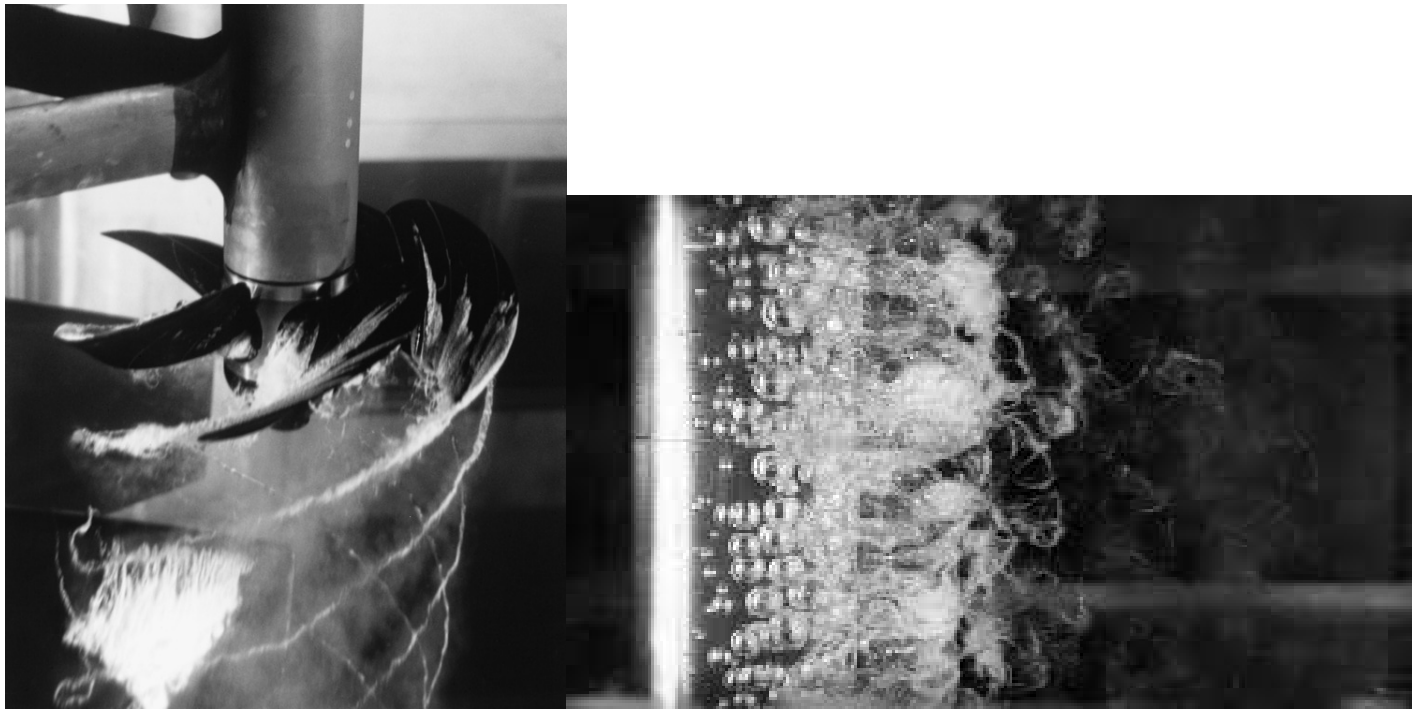

Multiphase flows occur in nature and industrial applications

- in high power ultrasonics
- to homogenize, or mix and break down particles
- to cavitate water purification devices
- for destruction of kidney stones via shock waves

Problem Statement

- Shock propagation in multiphase mixtures.
- Many applications : condensed phase mixtures, shock propagation in solid alloys, solid and liquid propellants as well as condensed solid explosives.
- Our problem is related to detonation problem with high explosives.
- Experimental works
  - in USA ; *Marsh : LASL Shock Hugoniot Data.*
  - in Russia ; *Bushman : Shock wave data base.*
  - This research area is closely related to the building of equations of state for condensed materials.
- Modeling efforts have been done in order to treat shock propagation in such mixtures.

Outline

First model

$$
\begin{aligned}
\frac{\partial \alpha_{1,2}}{\partial t} + u_I \frac{\partial \alpha_{1,2}}{\partial x} &= 0 + S^1_{1,2} \\
\frac{\partial [\alpha_{1,2}\rho_{1,2}]}{\partial t} + \frac{\partial [\alpha_{1,2}\rho u_{1,2}}{\partial x} &= 0 + S^2_{1,2} \\
\frac{\partial [\alpha_{1,2}\rho_{1,2}u_{1,2}]}{\partial t} + \frac{\partial [\alpha_{1,2}\left(\rho_{1,2}u^2_{1,2}+p_{1,2}\right)]}{\partial x} &= p_I \frac{\partial \alpha_{1,2}}{\partial x} + S^3_{1,2} \\
\frac{\partial [\alpha_{1,2}E_{1,2}]}{\partial t} + \frac{\partial [\alpha_{1,2}u_{1,2}\left(E_{1,2}+p_{1,2}\right)}{\partial x} &= u_I p_I \frac{\partial \alpha_{1,2}}{\partial x} + S^4_{1,2}
\end{aligned}
$$

Problems

- How to choose u_I, p_I ? modelisation problem
- non conservative products $u_I \dfrac{\partial \alpha}{\partial x}$: how to handle them ?

Another model : Baer and Nunziato, Int. J. of Multiphase Flows, vol 12, 1986

$$
\begin{aligned}
\frac{\partial \alpha_1}{\partial t} + u_I \frac{\partial \alpha_1}{\partial x} &= \mu \Delta p \\
\frac{\partial (\alpha\rho)_1}{\partial t} + \frac{\partial}{\partial x}\left((\alpha\rho u)_1\right) &= 0 \\
\frac{\partial (\alpha\rho u)_1}{\partial t} + \frac{\partial}{\partial x}\left((\alpha\rho u^2 + \alpha p)_1\right) &= p_I \frac{\partial \alpha_1}{\partial x} + \lambda \Delta u \\
\frac{\partial (\alpha\rho E)_1}{\partial t} + \frac{\partial}{\partial x}\left((\alpha u(\rho E + p)\right)_1 &= p_I u_I \frac{\partial \alpha_1}{\partial x} + \lambda p_I \Delta u + \mu u_I \Delta p
\end{aligned}
$$

$$
\begin{aligned}
\frac{\partial (\alpha\rho)_2}{\partial t} + \frac{\partial}{\partial x}\left((\alpha\rho u)_2\right) &= 0 \\
\frac{\partial (\alpha\rho u)_2}{\partial t} + \frac{\partial}{\partial x}\left((\alpha\rho u^2 + \alpha p)_2\right) &= p_I \frac{\partial \alpha_2}{\partial x} - \lambda \Delta u \\
\frac{\partial (\alpha\rho E)_2}{\partial t} + \frac{\partial}{\partial x}\left((\alpha u(\rho E + p)\right)_2 &= p_I u_I \frac{\partial \alpha_2}{\partial x} - \lambda p_I \Delta u - \mu u_I \Delta p
\end{aligned}
$$

with : interface quantities given by fluid
Extension by : R. Saurel–RA, JCP 1999 : Euler for each phase, interface terms : hyperbolic system, but not strictly hyperbolic, whatever the closure u_I, p_I.

The five-equation flow model for compressible two-phase problems

Equations for two-phase flows

$$\frac{\partial \alpha_1}{\partial t} + u\frac{\partial \alpha_1}{\partial x} = K(p,\rho_1,\rho_2,\alpha_1)\frac{\partial u}{\partial x}$$
$$\frac{\partial (\alpha\rho)_1}{\partial t} + \frac{\partial (\alpha\rho)_1 u}{\partial x} = 0$$
$$\frac{\partial (\alpha\rho)_2}{\partial t} + \frac{\partial (\alpha\rho)_2 u}{\partial x} = 0$$
$$\frac{\partial \rho u}{\partial t} + \frac{\partial (\rho u^2 + p)}{\partial x} = 0$$
$$\frac{\partial \rho E}{\partial t} + \frac{\partial u(\rho E + p)}{\partial x} = 0$$

where $\alpha, \rho, u, p, E(= e + \frac{1}{2}u^2)$ and e are the volume fraction, density, velocity, pressure, total energy and internal energy respectively.

$$K(p,\rho_1,\rho_2,\alpha_1) = \frac{\rho_2 c_2^2 - \rho_1 c_1^2}{\frac{\rho_1 c_1^2}{\alpha_1} + \frac{\rho_2 c_2^2}{\alpha_2}}$$

.

Mixture Stiffened Gas Equation of State

The pure phase's SG EOS :

$$p_k = (\gamma_k - 1)\rho_k e_k - \gamma_k p_{\infty k}$$

The mixture internal energy :

$$\rho e = (\alpha\rho)_1 e_1 + (\alpha\rho)_2 e_2$$

$$\rho e = \alpha_1 \frac{p_1 + \gamma_1 p_{\infty 1}}{(\gamma_1 - 1)} + \alpha_2 \frac{p_2 + \gamma_2 p_{\infty 2}}{(\gamma_2 - 1)}$$

Kapila A, Meniko R, Bdzil J, Son S and Stewart D 2001 Phys. Fluids **13** 3002

What about jump relations ?

Recall : A system of conservation laws, Hugoniot jump conditions

$$\frac{\partial U}{\partial t} + \nabla \cdot F = 0$$

$$F(U_L) - \sigma U_L = F(U_R) - \sigma U_R$$

Single phase : Hugoniot

Shock : Left $\rho_L, \tau_L, u_L, p_L, e_L$; Right $\rho_R, \tau_R, u_R, p_R, e_R$

$$(e_L - e_R) + \frac{p_L + p_R}{2}(\tau_L - \tau_R) = 0; \qquad (p_L - p_R)(\tau_L - \tau_R) + (u_L - u_R)^2 = 0$$

$$\Delta e + \bar{p}\Delta\tau = 0; \qquad \Delta p \Delta\tau + \Delta u^2 = 0$$

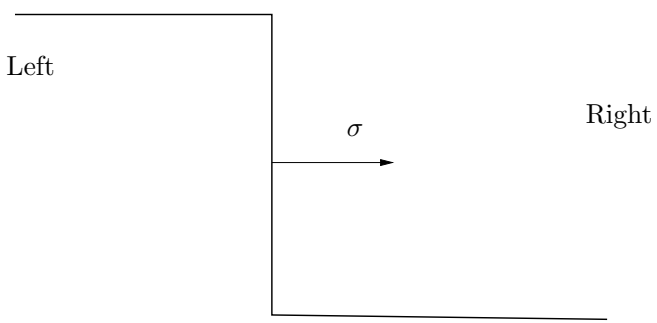

What about jump relations ?

Two phases, one realisation

- Phase 1 Shock : Left $\rho_{L,1}, \tau_{L,1}, u_{L,1}, p_{L,1}, e_{L,1}$; Right $\rho_{R,1}, \tau_{R,1}, u_{R,1}, p_{R,1}, e_{R,1}$

$$\Delta e_1 + \bar{p}_1 \Delta \tau_1 = 0; \qquad \Delta p_1 \Delta \tau_1 + \Delta u_1^2 = 0$$

- Phase 2 Shock : Left $\rho_{L,2}, \tau_{L,2}, u_{L,2}, p_{L,2}, e_{L,2}$; Right $\rho_{R,2}, \tau_{R,2}, u_{R,2}, p_{R,2}, e_{R,2}$

$$\Delta e_2 + \bar{p}_2 \Delta \tau_2 = 0; \qquad \Delta p_2 \Delta \tau_2 + \Delta u_2^2 = 0$$

- impose : $p_{L,1} = p_{L,2} = p_L$ and $p_{R,1} = p_{L,2} = p_R$

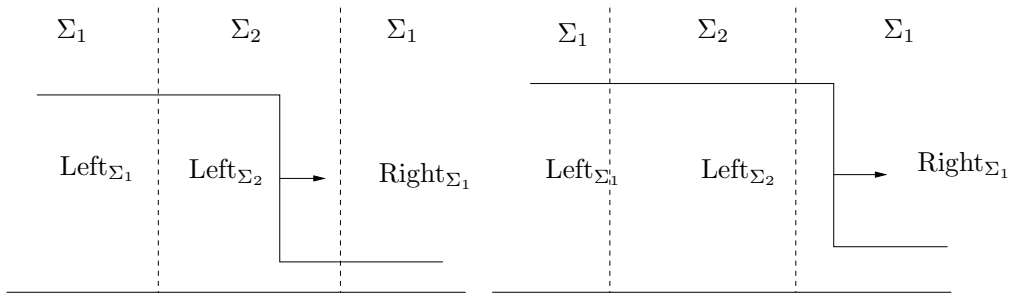

- The shock propagates through materials, speed depends on materials.
- Very similar to linear accoustics in random media

$$\frac{1}{c^2} = \frac{\alpha_1}{c_1^2} + \frac{\alpha_2}{c_2^2}$$

Case Study : Two-phase flow problem

- Phase 1 corresponds to epoxy, which is the most compressible phase with the lowest speed of sound and supports a shock wave.
- Phase 2 corresponds to periclase, which is the less compressible.

Epoxy-periclase mixture initial data

Mixture	$\rho_m^0 (g/cm^3)$ (g/cm^3)	α_1^0	ρ_1^0/ρ_2^0	Z_1^0/Z_2^0
Epoxy-periclase	2.219	0.56	0.33	0.14

Pure material EOS parameters

	p_∞ bar	γ	ρ_0 (g/cm^3)	c_0 (cm/ms)	s	$Z_0 = \rho_0 c_0$ $g/(cm^2 ms)$
Epoxy	53000	2.43	1.185	280	1.44	331.8
Periclase	457000	3.49	3.584	660	1.37	2365.4

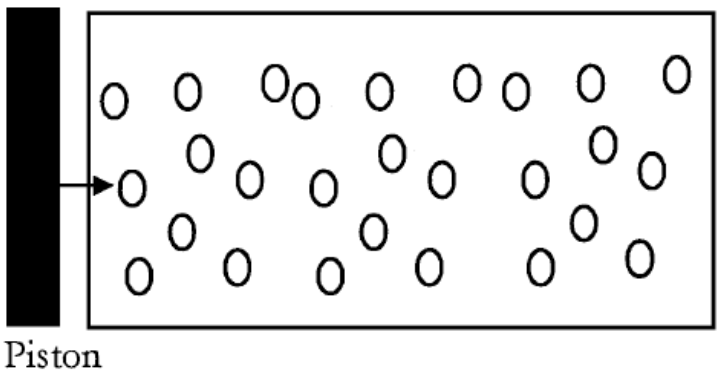

Experimental Data

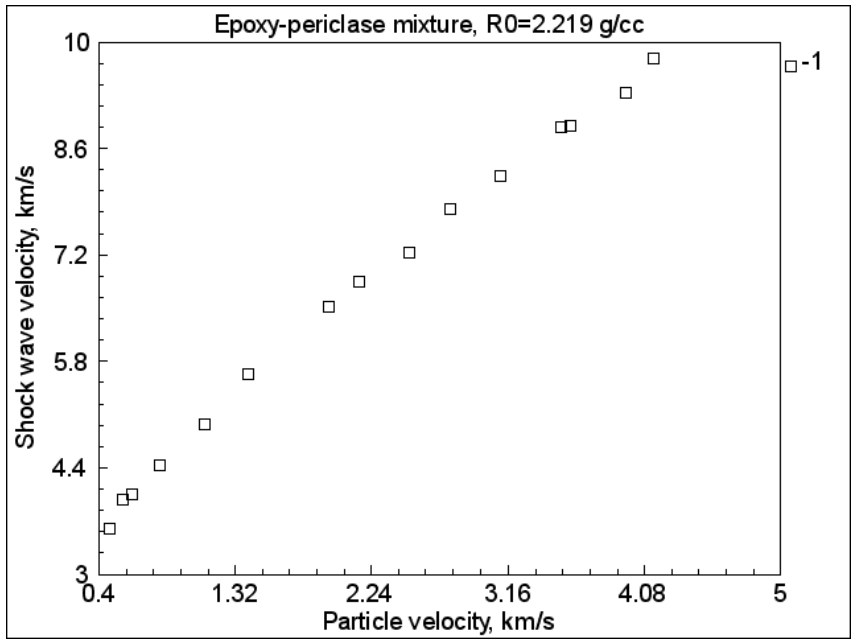

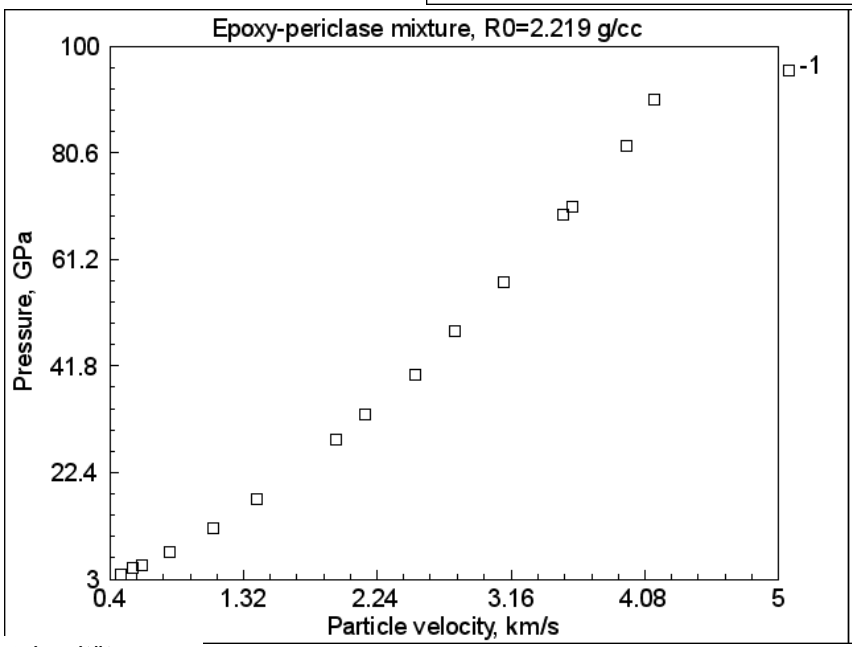

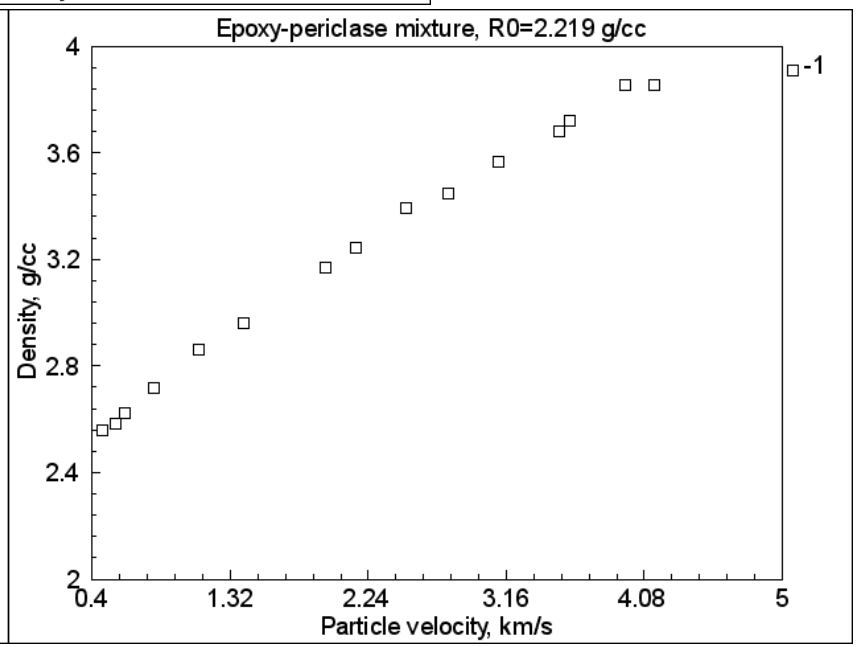

Outline

STONY BROOK UNIVERSITY

Front Tracking (*FronTier* simulation package)

- to achieve resolution of steep and sharp density gradients
- treat discontinuities as moving internal boundaries, and the jump conditions are imposed

A mature, production-quality multiphysics simulation package, supports a range of physics, each with its own validation and verification studies.

Performance of *FronTier*

- FronTier scales to the entire system on Argonne's IBM Blue Gene/P supercomputer - 62% efficiency on 163,840 cores
- Innovative and Novel Computational Impact on Theory and Experiment Awards
  - "Stochastic (w*) Convergence for Turbulent Combustion", 2012
  - "Uncertainty Quantification for Turbulent Mixing", 2011

Front Tracking method

- an adaptive computational method that provides sharp resolution of a wave front by tracking the interfaces between distinct materials.
- implemented in code *FronTier*.

FronTier

solves the equations with the following main steps :

1. interface propagation.
2. interpolation reconstruction.
3. interior states update.

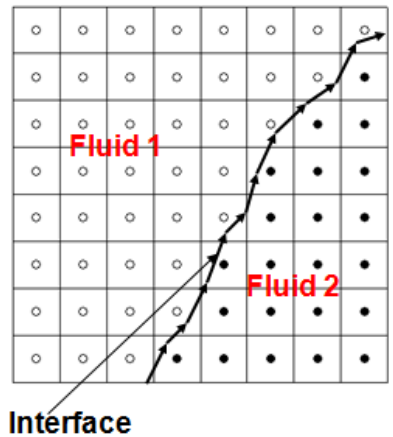

Interface propagation step

Interface states are reconstructed from the interpolation of real and ghost states.

- A Riemann problem with left, right interface states as its data is solved to determine the wave speed.
- A new position for the point is determined from the equation

$$\mathbf{x}^{\text{new}} = \mathbf{x}^{\text{old}} + V\Delta t\mathbf{n}$$

V : the wave speed
$\mathbf{n}$: the normal direction to the interface at the point
Δt : the time step size

In the interior state update step

Fifth Order Weighted Essentially non-oscillatory (WENO) scheme :

- achieves high order accuracy and non-oscillatory property near discontinuities
- has been widely used to solve compressible flow equations

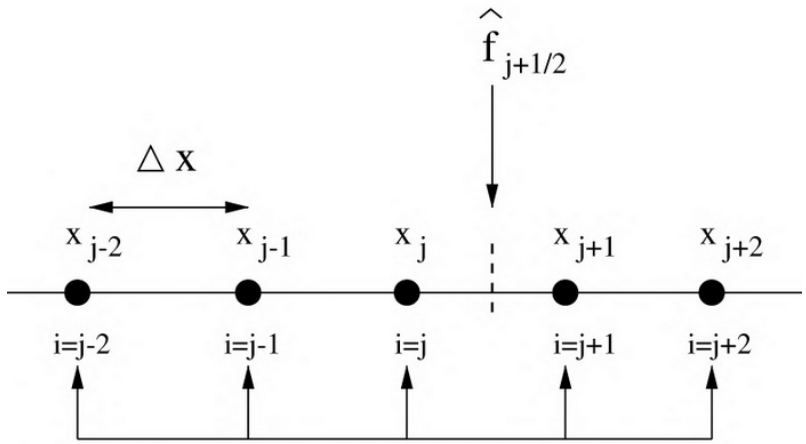

Here we have three stencils and each stencil has three points. The approximations are :

$$f_{i+1/2}^{(0)} = \frac{1}{3} f_{i-2} - \frac{7}{6} f_{i-1} + \frac{11}{6} f_i$$

$$f_{i+1/2}^{(1)} = -\frac{1}{6} f_{i-1} + \frac{5}{6} f_i + \frac{1}{3} f_{i+1}$$

$$f_{i+1/2}^{(2)} = \frac{1}{3} f_i + \frac{5}{6} f_{i+1} - f_{i+2}$$

$$f_{i+1/2} = \gamma_0 f_{i+1/2}^{(0)} + \gamma_1 f_{i+1/2}^{(1)} + \gamma_2 f_{i+1/2}^{(2)}$$

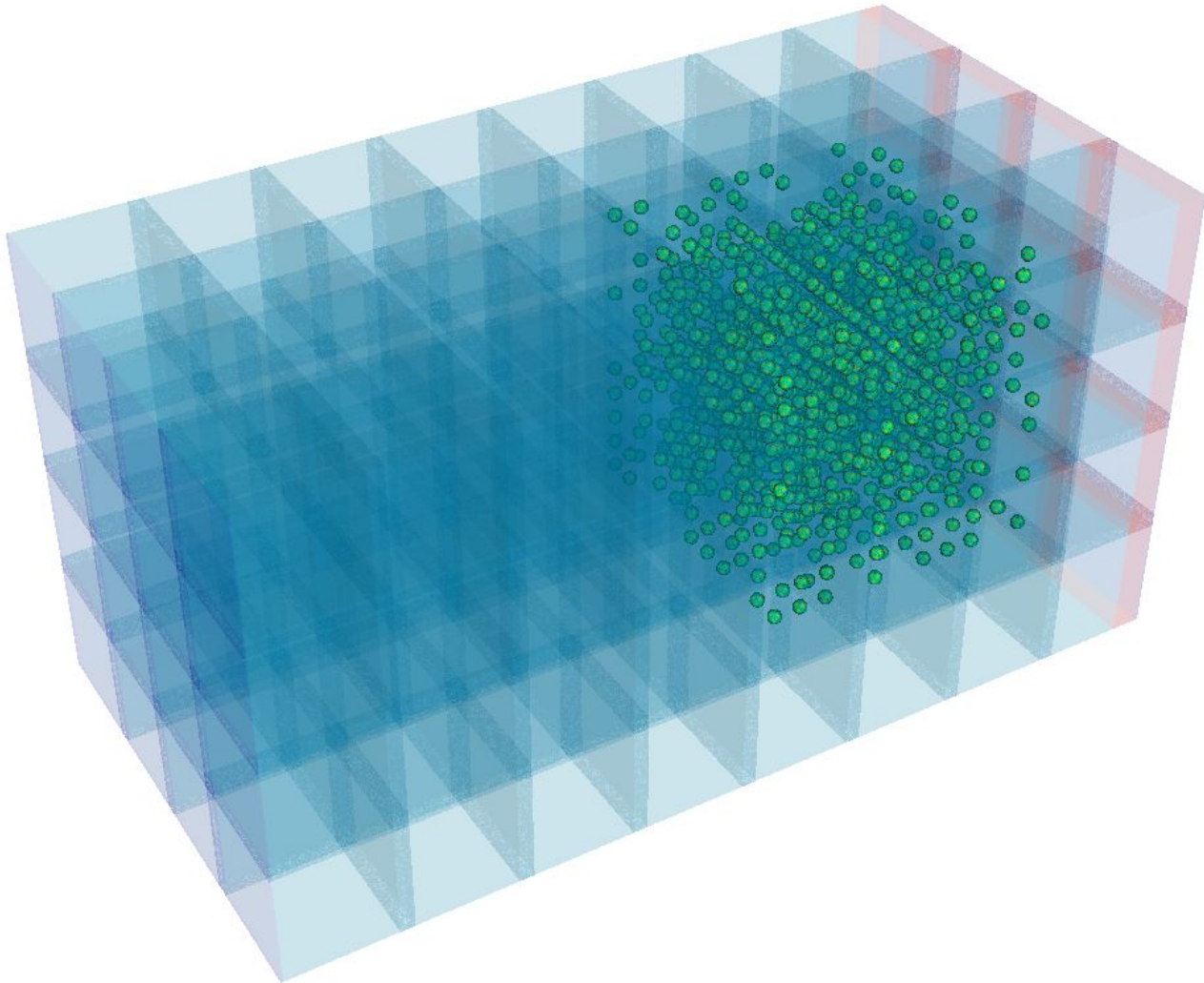

Comparison with numerical simulation

Theoretical speed of shock

$$\sigma_{\text{theory}} = \frac{(\rho_L u_L^2 + p_L) - (\rho_R u_R^2 + p_R)}{\rho_L u_L + \rho_R u_R}$$

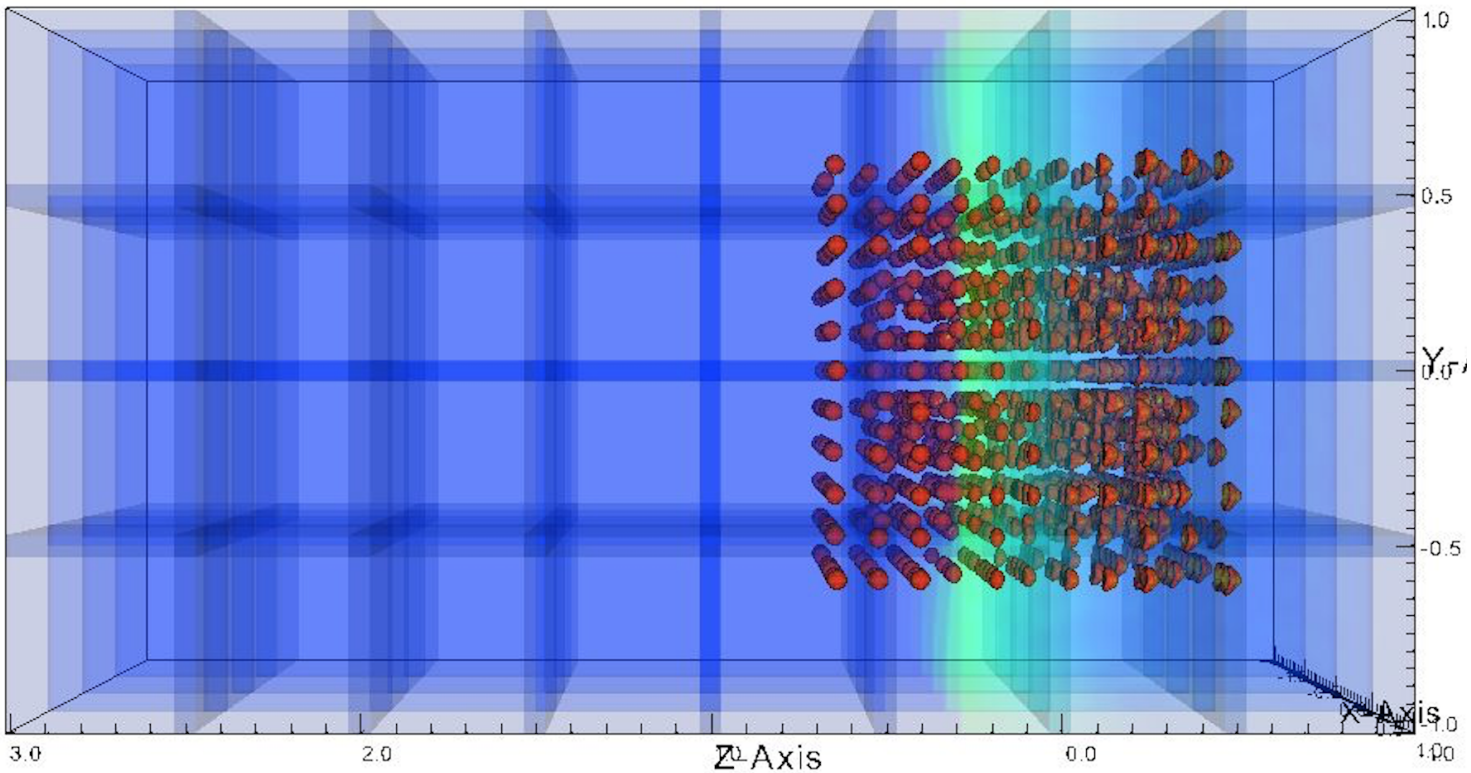

Comparison with numerical simulation

Theoretical speed of shock

$$\sigma_{\text{theory}} = \frac{(\rho_L u_L^2 + p_L) - (\rho_R u_R^2 + p_R)}{\rho_L u_L + \rho_R u_R}$$

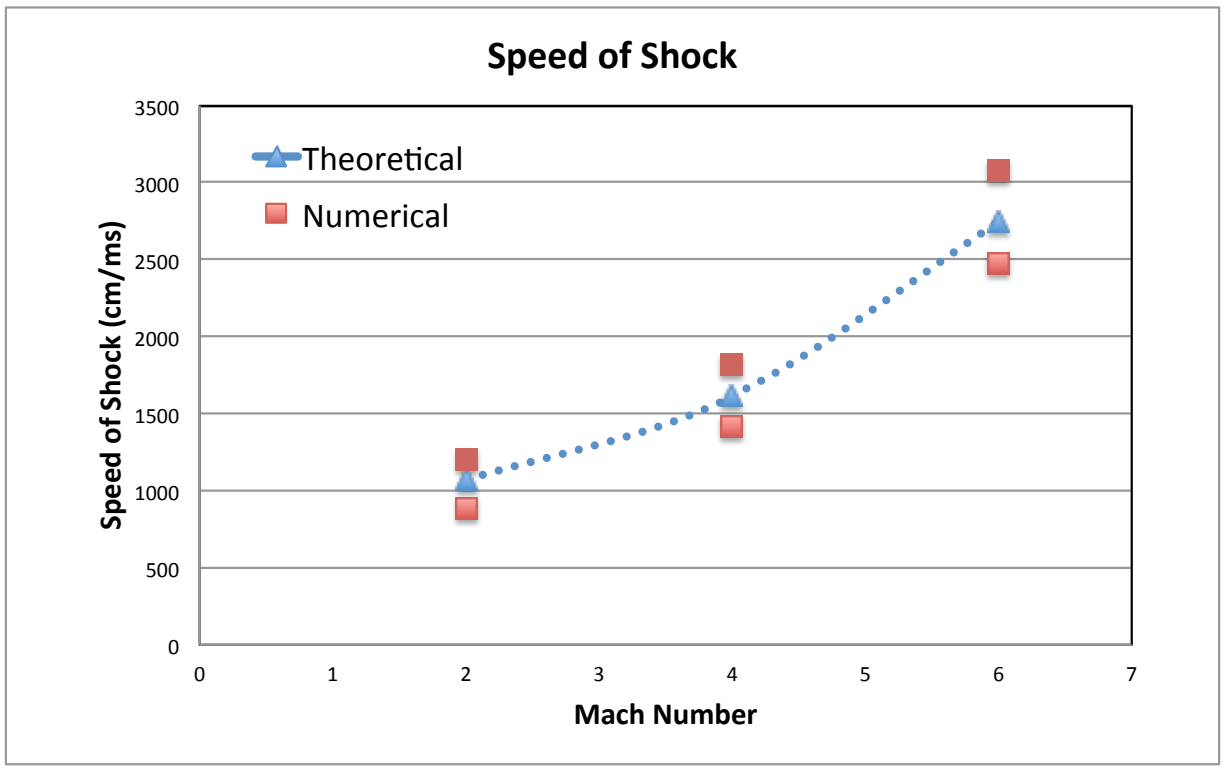

Outline

- Cloud interaction parameter :

$$\beta = \alpha_0 \left(\frac{A_0}{R_0} \right)^2$$

- Initial bubble fraction of the cloud :

$$\alpha_0 = \frac{1}{V_c} \sum_{i=1}^{N} \frac{4}{3} \pi R_i^3$$

- Initial radius of the cloud :

$$A_0 = \sqrt[3]{\sum_{i=1}^{N} R_i^3}$$

- Initial average radius of the bubbles within the cloud :

$$R_0 = \frac{1}{N} \sum_{i=1}^{N} R_i$$

Cloud interaction parameter

Cloud interaction parameter β for $1331 = 11^3$

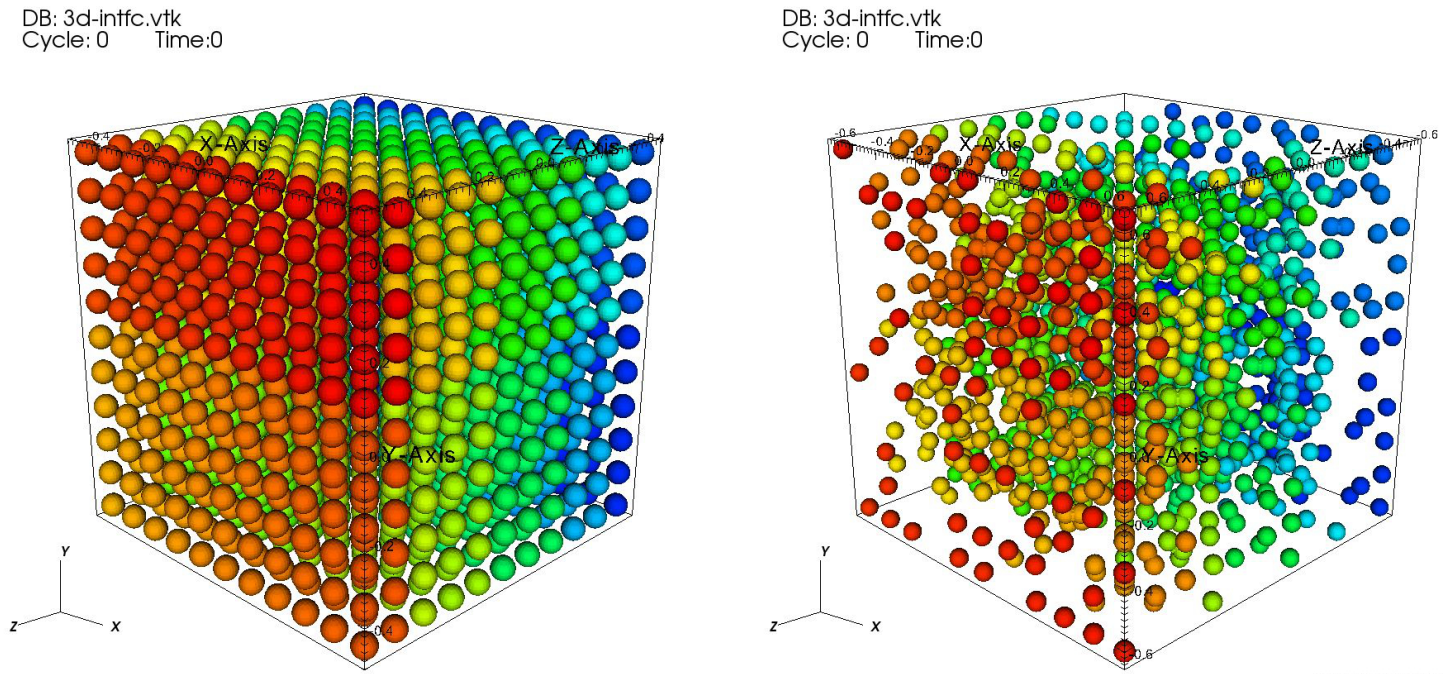

Figure: Initialization of regular/random distribution of 1331 bubbles.

Validation

Comparison of experiment to FronTier simulations

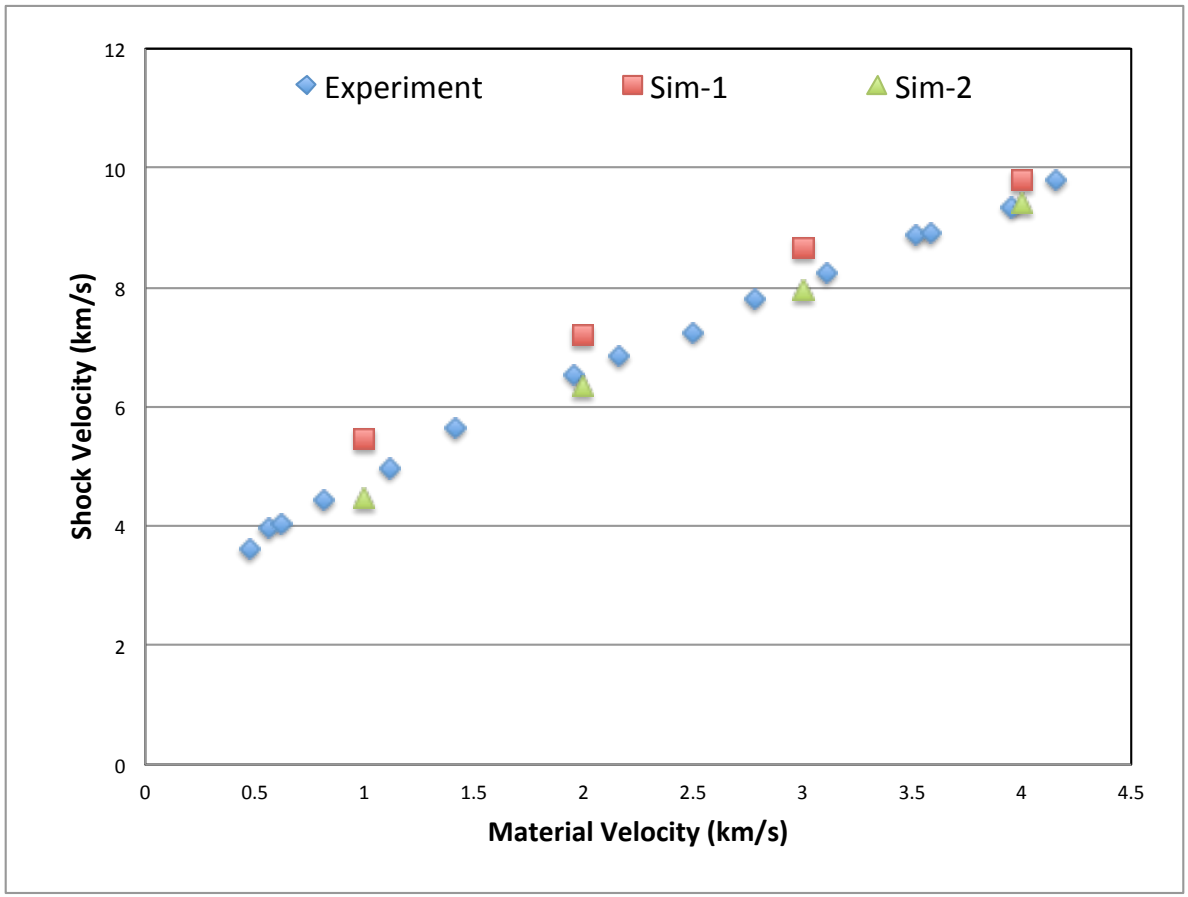

Distance between bubbles

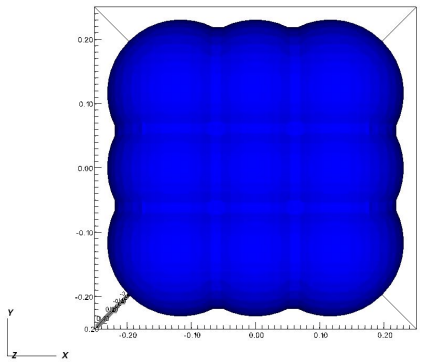

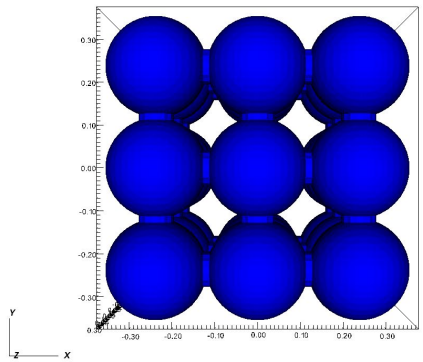

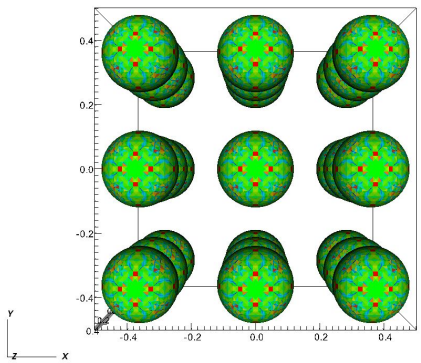

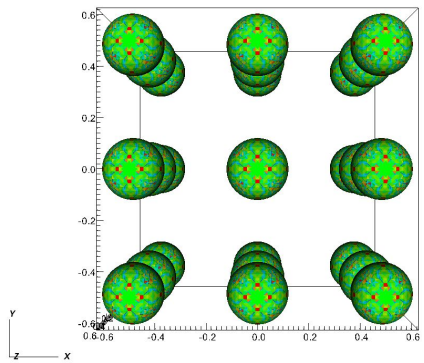

Pressure at time 0.4 μs for $\beta = 125, 15, 5, 1$

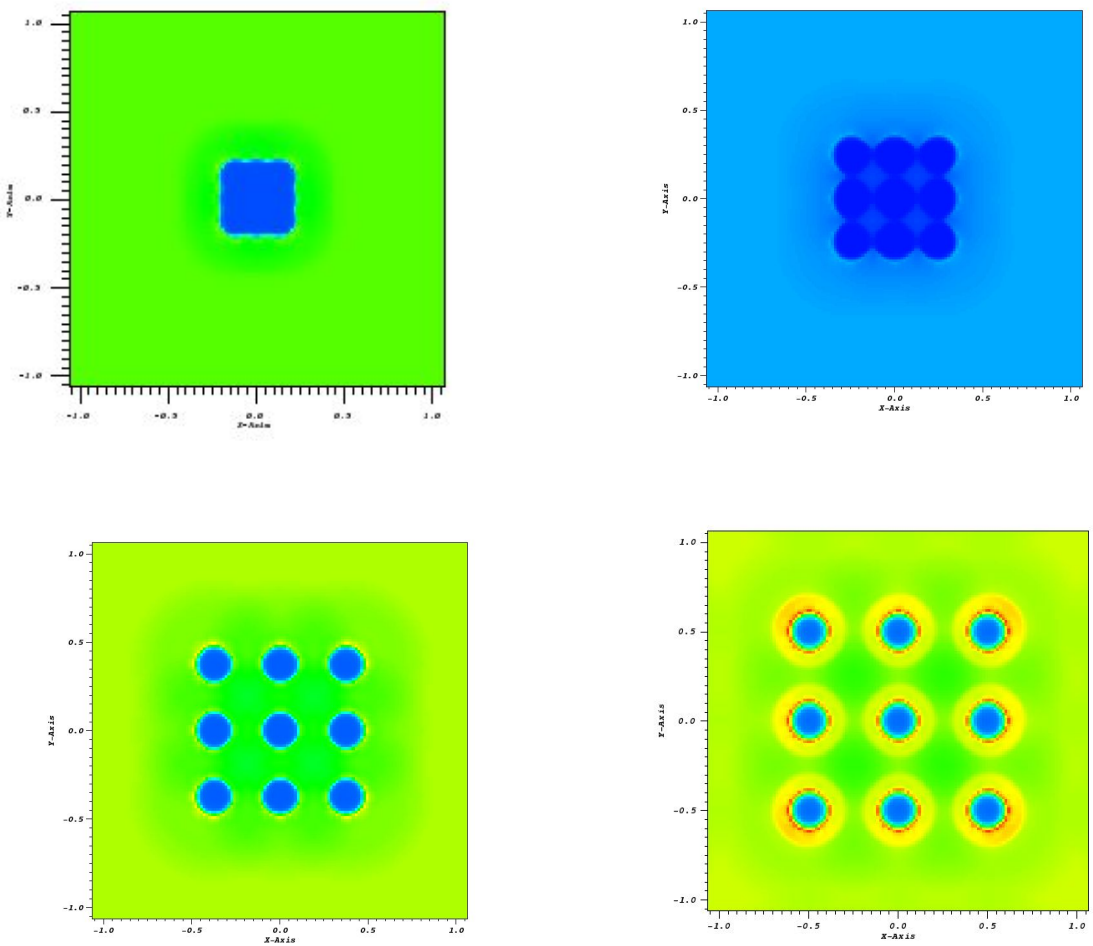

Uncertainty Quantification (UQ) Tools

- Scientific Discovery through Advanced Computing (SciDAC)
- **QUEST** - is a SciDAC Institute that is focused on UQ in large-scale scientific computations. (http ://www.quest-scidac.org/)
- UQ software tools that are included in the QUEST
  1. UQTk (SNL) (http ://www.sandia.gov/UQToolkit) provides routines for evaluating algebraic expressions and transcendental functions of random variables represented with Polynomial Chaos expansions.
  2. DAKOTA (SNL) (http ://dakota.sandia.gov) provides a variety of non-intrusive algorithms for design optimization, model calibration, uncertainty quantification, global sensitivity analysis, solution verification, and parameter studies.
  3. QUESO (UT) provides statistical algorithms for Bayesian inference, model calibration, model validation, and decision making under uncertainty.
  4. GPMSA (LANL) allows for global sensitivity analysis, forward propagation of uncertainty, model calibration/parameter estimation, and predictions with uncertainty.

UQ Toolkit (UQTk)

- is a lightweight C++ library, offers tools for (non)intrusive uncertainty propagation.
- The technique for forward UQ is the spectral Polynomial Chaos expansions (PCEs) : allows for
  - efficient uncertainty propagation
  - very fast global sensitivity analysis
  - cheap surrogate model construction

Generic Workflow

1. Generate parameter samples to run the forward model at, for PC construction
2. Run the black-box model (*FronTier*)
3. Obtain PCE for the model
4. Postprocessing : global sensitivity analysis

PC Type	Domain	Density $w(\xi)$	Polynomial	Free parameters
Gauss-Hermite	$(-\infty, +\infty)$	$\frac{1}{\sqrt{2\pi}} e^{-\frac{\xi^2}{2}}$	Hermite	none
Legendre-Uniform	$[-1, 1]$	$\frac{1}{2}$	Legendre	none
Gamma-Laguerre	$[0, +\infty)$	$\frac{x^\alpha e^{-\xi}}{\Gamma(\alpha+1)}$	Laguerre	$\alpha > -1$
Beta-Jacobi	$[-1, 1]$	$\frac{(1+\xi)^\alpha (1-\xi)^\beta}{2^{\alpha+\beta+1} B(\alpha+1, \beta+1)}$	Jacobi	$\alpha > -1, \beta > -1$

Global sensitivity analysis

- maximum pressure, velocity depend on the distance between bubbles

Convergence of pressure : PDFs & CDFs

- From a single deterministic simulation, extract a Probability Distribution Function (PDF) by binning results from a space time neighborhood of the convergence point.
- The binned state values constitute a discrete set of solution values which define an approximate PDF.
- The convergence of the associated cumulative distribution functions (CDFs) are assessed by standard function space metrics.
- Convergence is to a probability distribution indexed by space and time, also known as a Young measure.
- We study integrated convergence through an L_1 norm (relative to integration both in solution state variables and over space-time) for the CDFs.

Explore the consequence of varying the definitions used for convergence.

- the mesh,
- PDF vs. CDF,
- the size of the supercell used to define the statistical PDF.

Pressure at the midplane x, z midplane

For each supercell, we bin the shock velocity values into 5 bins, and count the number of values lying in each bin, to obtain a probability.

Coarse : $\Delta x = 0.03125$

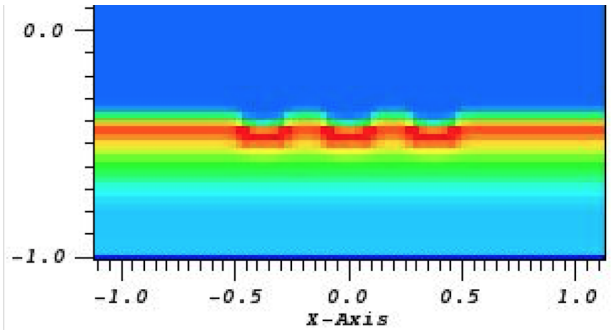

Medium : $\Delta x = 0.015625$

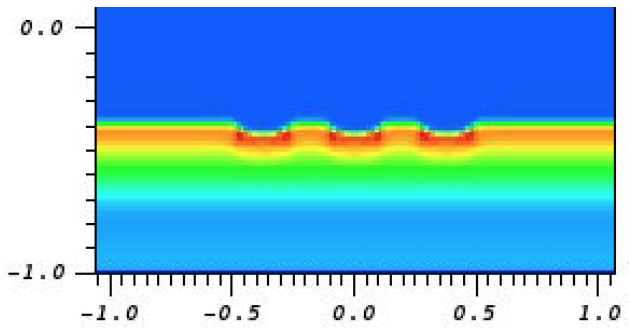

Fine : $\Delta x = 0.0078125$

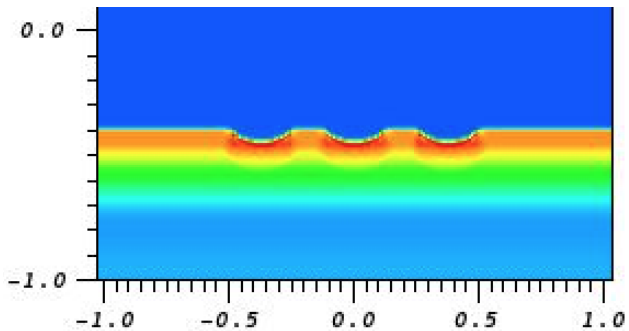

Supercell resolution

- The coarsest grid has for each supercell a resolution

a) 2×4 supercell grid ; 16×16

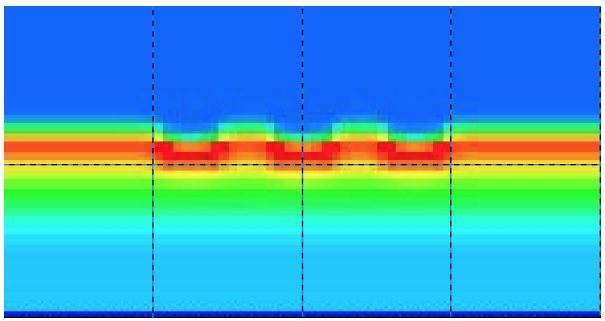

b) 1×4 supercell grid ; 32×16

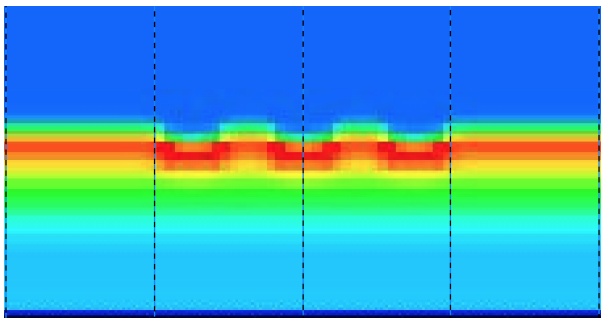

- The supercell partition is unchanged for the medium and fine grids, the number of cells in each direction increases by factors of 2 and 4.

Norm comparison of convergence

Norm comparison of convergence for pressure PDFs and CDFs at fixed values of y, t. In each supercell, an L_1 norm is applied to the difference of the PDFs or CDFs.

coarse grid supercell size mesh comparison	a) 16×16 L_1	b) 32×16 L_1
CDFs : coarse to fine	0.0464	0.0139
CDFs : medium to fine	0.0218	0.0053
PDFs : coarse to fine	0.028	0.0217
PDFs : medium to fine	0.0176	0.0039

Observed

a coarsening of the supercell resolution (increase of the supercell size) to 32×16 coarse grid cells per supercell is needed to obtain single digit convergence errors.

Outline

- presented a method for the approximation of a compressible, hyperbolic multiphase problem given by Kapila five equation model
- Derivation/justification of jump relations

Ongoing Work

- Take into account more complex (spherical, cylindrical) cloud
- Generate and initialize numerical simulations via Gaussian random field
- Find the mesh that gives acceptable accuracy for certain bubbles $\Rightarrow$ statistical convergence...

CSCS-Piz Daint - 8th place in TOP500 Lists (SC November 2016)

- Cray supercomputer installed at the Swiss National Supercomputing Centre (CSCS)
- The second most energy-efficient supercomputer in the TOP500, with a rating of 7.45 gigaflops/watt
- The only system on the list equipped with the new P100 GPUs. It is a 3.3-petaflop cluster of DGX-1 servers that delivers 9.46 gigaflops/watt.

Rank	Site	System	Cores	Rmax (TFlop/s)	Rpeak (TFlop/s)	Power (kW)
1	National Supercomputing Center in Wuxi China	**Sunway TaihuLight** - Sunway MPP, Sunway SW26010 260C 1.45GHz, Sunway NRCPC	10,649,600	93,014.6	125,435.9	15,371
2	National Super Computer Center in Guangzhou China	**Tianhe-2 (MilkyWay-2)** - TH-IVB-FEP Cluster, Intel Xeon E5-2692 12C 2.200GHz, TH Express-2, Intel Xeon Phi 31S1P NUDT	3,120,000	33,862.7	54,902.4	17,808
3	DOE/SC/Oak Ridge National Laboratory United States	**Titan** - Cray XK7 , Opteron 6274 16C 2.200GHz, Cray Gemini interconnect, NVIDIA K20x Cray Inc.	560,640	17,590.0	27,112.5	8,209
4	DOE/NNSA/LLNL United States	**Sequoia** - BlueGene/Q, Power BQC 16C 1.60 GHz, Custom IBM	1,572,864	17,173.2	20,132.7	7,890
5	DOE/SC/LBNL/NERSC United States	**Cori** - Cray XC40, Intel Xeon Phi 7250 68C 1.4GHz, Aries interconnect Cray Inc.	622,336	14,014.7	27,880.7	3,939
6	Joint Center for Advanced High Performance Computing Japan	**Oakforest-PACS** - PRIMERGY CX1640 M1, Intel Xeon Phi 7250 68C 1.4GHz, Intel Omni-Path Fujitsu	556,104	13,554.6	24,913.5	2,719
7	RIKEN Advanced Institute for Computational Science (AICS) Japan	K computer, SPARC64 VIIIfx 2.0GHz, Tofu interconnect Fujitsu	705,024	10,510.0	11,280.4	12,660
8	Swiss National Supercomputing Centre (CSCS) Switzerland	**Piz Daint** - Cray XC50, Xeon E5-2690v3 12C 2.6GHz, Aries interconnect , NVIDIA Tesla P100 Cray Inc.	206,720	9,779.0	15,988.0	1,312